A high resolution optical vector network analyzer based on a wideband and wavelength-tunable optical single-sideband modulator

Zhenzhou Tang,[1] Shilong Pan,[1,*] and Jianping Yao[1,2]

[1]*College of Electronic and Information Engineering, Nanjing University of Aeronautics and Astronautics, Nanjing, 210016, China*

[2]*Microwave Photonics Research Laboratory, School of Electrical Engineering and Computer Science University of Ottawa, Ottawa, ON, K1N 6N5, Canada*

[*] *pans@ieee.org*

Abstract: A high resolution optical vector network analyzer (OVNA) implemented based on a wideband and wavelength-tunable optical single-sideband (OSSB) modulator is proposed and experimentally demonstrated. The OSSB modulation is achieved using a phase modulator and a tunable optical filter with a passband having two steep edges and a flat top. Wideband and wavelength-tunable OSSB modulation is achieved. The incorporation of the OSSB modulator into the OVNA is experimentally evaluated. The measurement of the magnitude and phase response of an ultra-narrow-band fiber Bragg grating (FBG) and that of the stimulated Brillouin scattering (SBS) in a single-mode fiber is performed. A measurement resolution as high as 78 kHz is achieved.

OCIS codes: (070.1170) Analog optical signal processing; (999.9999) Single sideband; (999.9999) Microwave photonics.

References and links

1. T. Niemi, M. Uusimaa, and H. Ludvigsen, "Limitations of phase-shift method in measuring dense group delay ripple of fiber Bragg gratings," IEEE Photon. Technol. Lett. **13**(12), 1334–1336 (2001).
2. G. D. VanWiggeren, A. R. Motamedi, and D. M. Barley, "Single-scan interferometric component analyzer," IEEE Photon. Technol. Lett. **15**(2), 263–265 (2003).
3. J. E. Román, M. Y. Frankel, and R. D. Esman, "Spectral characterization of fiber gratings with high resolution," Opt. Lett. **23**(12), 939–941 (1998).
4. R. Hernandez, A. Loayssa, and D. Benito, "Optical vector network analysis based on single-sideband modulation," Opt. Eng. **43**(10), 2418–2421 (2004).
5. A. Loayssa, R. Hernández, D. Benito, and S. Galech, "Characterization of stimulated Brillouin scattering spectra by use of optical single-sideband modulation," Opt. Lett. **29**(6), 638–640 (2004).
6. M. Sagues and A. Loayssa, "Spectral characterisation of polarisation dependent loss of optical components using optical single sideband modulation," Electron. Lett. **47**(1), 47–48 (2011).
7. M. Sagues and A. Loayssa, "Swept optical single sideband modulation for spectral measurement applications using stimulated Brillouin scattering," Opt. Express **18**(16), 17555–17568 (2010).
8. G. H. Smith, D. Novak, and Z. Ahmed, "Overcoming chromatic-dispersion effects in fiber-wireless systems incorporating external modulators," IEEE Trans. Microw. Theory Tech. **45**(8), 1410–1415 (1997).
9. J. Park, W. V. Sorin, and K. Y. Lau, "Elimination of the fibre chromatic dispersion penalty on 1550nm millimetre-wave optical transmission," Electron. Lett. **33**(6), 512–513 (1997).
10. S. R. Blais and J. P. Yao, "Optical single sideband modulation using an ultranarrow dual-transmission-band fiber Bragg grating," IEEE Photon. Technol. Lett. **18**(21), 2230–2232 (2006).
11. G. Ning, J. Q. Zhou, L. Cheng, S. Aditya, and P. Shum, "Generation of different modulation formats using Sagnac fiber loop with one electroabsorption modulator," IEEE Photon. Technol. Lett. **20**(4), 297–299 (2008).
12. Z. Li, H. Chi, X. Zhang, and J. P. Yao, "Optical single-sideband modulation using a fiber-Bragg-grating-based optical Hilbert transformer," IEEE Photon. Technol. Lett. **23**(9), 558–560 (2011).
13. A. Schoof, J. Grünert, S. Ritter, and A. Hemmerich, "Reducing the linewidth of a diode laser below 30 Hz by stabilization to a reference cavity with a finesse above 10(5)," Opt. Lett. **26**(20), 1562–1564 (2001).
14. J. Cliche, Y. Painchaud, C. Latrasse, M. Picard, I. Alexandre, and M. Têtu, " Ultra-Narrow Bragg grating for active semiconductor laser linewidth reduction through electrical feedback," in Bragg Gratings, Photosensitivity, and Poling in Glass Waveguides, OSA Technical Digest (CD) (Optical Society of America, 2007), paper BTuE2.

#159312 - $15.00 USD Received 2 Dec 2011; revised 29 Feb 2012; accepted 1 Mar 2012; published 6 Mar 2012

15. G. P. Agrawal, *Nonlinear Fiber Optics*, 3rd ed. (Academic Press, New York, 2006).

1. Introduction

The measurement of the magnitude and phase response of an optical component is essential for both device characterization and system design. Conventionally, two main approaches are used to analyze the transmission or reflection response of an optical component, namely the modulation phase-shift approach [1] and the interferometry approach [2]. Recently, the implementation of an optical vector network analyzer (OVNA) based on optical single-sideband (OSSB) modulation to measure the magnitude and phase response of an optical component by sweeping the frequency of one optical sideband was proposed [3–7]. The key advantage of this approach is that very high resolution, potentially at femtometer level, can be achieved.

To implement an OSSB-based OVNA, the key is to realize wideband and wavelength-tunable OSSB modulation. Numerous techniques have been reported to implement OSSB modulation [7–12], but few can achieve wideband and wavelength-tunable operation. For instance, a dual-port Mach-Zehnder modulator (MZM) can be used to perform OSSB modulation [8], but the configuration always requires an electrical hybrid coupler to introduce a $\pi/2$-phase shift between the RF signals introduced to the two RF ports. Since the bandwidth of a hybrid coupler is usually limited, the entire bandwidth of the scheme is usually small. A uniform fiber Bragg grating (FBG) [8] having a deep notch in the transmission response can be used to attenuate one of the two sidebands produced by conventional intensity or phase modulation. However, a uniform FBG always has a relatively large bandwidth, it is difficult to remove effectively one sideband without affecting the optical carrier and the other sideband. In addition, the tuning range of a FBG is very small, of about several nm, which cannot meet the requirement of an OVNA for large wavelength range measurement. OSSB modulation can also be realized by other techniques, such as the employment of an equivalent-phase-shift (EPS) FBG followed by a uniform FBG [9], an EAM-loop [10] or an optical Hilbert transformer [11]. Again, the bandwidth is small. In addition, the stability of the systems is usually poor since optical interference exists. Recently, OSSB modulation based on stimulated Brillouin scattering (SBS) is proposed and applied for optical vector network analysis [7], but two RF sources have to be used, which increases the complexity and cost.

In this paper, we propose and experimentally demonstrate a high resolution OVNA based on a wideband and wavelength tunable OSSB modulator. The key device in the OSSB modulator is a tunable optical filter which should have a passband with two steep edges and a flat-top, enabling a wideband and wavelength-tunable operation, which is highly desirable for an OVNA. In the experiment, a tunable optical filter with an edge slope of 230 dB/nm is employed. A wideband OSSB modulation from 11 to 40 GHz with an unwanted sideband suppression over 20 dB is achieved within 1535-1565 nm. Based on the proposed OSSB modulation scheme, an OVNA is constructed and its performance is evaluated. The measurement of the amplitude and phase response of an ultra-narrow band FBG and that of the SBS in a SMF is performed. A resolution as high as 78 kHz is achieved, which is much higher than a conventional OVNA based on the interferometry method.

2. Principle

Figure 1 shows the proposed OSSB modulator and its incorporation in an OVNA for high resolution vector network analysis. An optical carrier with a frequency of f_c from a tunable laser source (TLS) is modulated by a RF signal at f_m from an electrical vector network analyzer (EVNA) to produce an optical double-sideband (ODSB) signal. Then, the ODSB signal is sent to a tunable optical filter. Due to the steep edges and the flat top of the tunable optical filter, one sideband of the ODSB signal is effectively suppressed while the optical carrier and the other sideband are not affected. An OSSB signal is thus generated and is sent to a device-under-test (DUT). The remaining sideband would undergo amplitude and phase

#159312 - $15.00 USD Received 2 Dec 2011; revised 29 Feb 2012; accepted 1 Mar 2012; published 6 Mar 2012

changes due to the frequency response of the DUT at $f_c + f_m$. Then, the optical signal is converted into an electrical signal at a photodetector (PD), where the amplitude and phase information of the sideband is converted into the amplitude and phase changes of the generated electrical signal. When the electrical signal is fed back to the input port of the EVNA, the obtained electrical response at f_m represents the optical response of the DUT at $f_c + f_m$. Therefore, by sweeping the frequency of the RF signal from the EVNA, the optical phase and amplitude response of the DUT is obtained [3]. It should be noted that the EVNA can reach a spectral resolution as high as several Hz, so the resolution of the OVNA is mainly determined by the linewidth of the TLS. Recently, a diode laser with 10-Hz-level linewidth was reported [13], so the OVNA can potentially reach a resolution of tens of Hz.

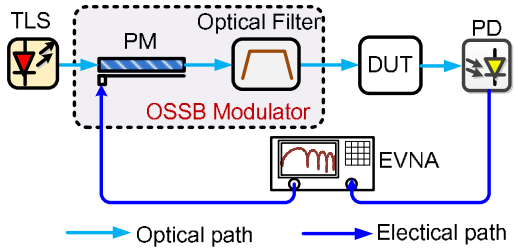

Fig. 1. The optical vector network analyzer based on the proposed optical single-sideband modulation scheme. TLS: tunable laser source, PM: phase modulator, DUT: device under test, PD: photodetector, EVNA: electrical vector network analyzer.

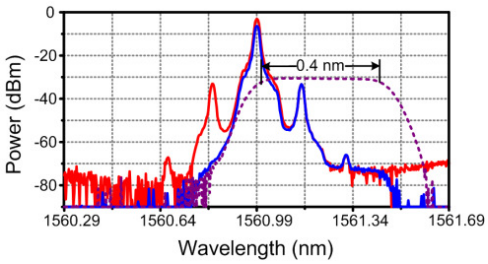

Fig. 2. Optical single-sideband signal generation using an optical filter with a passband having steep edges and a flat top. Dash line: the transmission spectrum of the optical filter; red line: the optical spectrum of the ODSB signal; and blue line: the optical spectrum of the generated OSSB signal.

The key device in the OVNA is the OSSB modulator, which is implemented using a phase modulator (PM) and a tunable optical bandpass filter. The PM is used to generate optical double-sideband (ODSB) modulation, which can also be replaced by an intensity modulator. It is known that the use of a PM would provide better performance due to its low insertion loss and bias-drift-free operation. The tunable optical filter is used to remove one sideband from the ODSB signal. A typical transmission response of the optical filter is shown as the dashed line in Fig. 2. When the optical carrier is located at the edge of the transmission band of the optical filter, as shown in Fig. 2, one sideband would experience a large optical loss and will be filtered out while the optical carrier and the other sideband are kept. Thus, OSSB modulation is achieved. As an example, if a RF signal at 20 GHz is applied to the PM, at the output of the optical filter an OSSB signal is generated, with the spectrum shown as the blue line in Fig. 2. As can be seen a sideband suppression as large as 40 dB is obtained. The bandwidth of the OSSB modulator is determined mainly by the spectral characteristics of the optical filter. Given an optical filter with an edge slope of k dB/nm and a 1-dB bandwidth of b nm, the generated OSSB signal at around 1550 nm can have a frequency in the range from $125a/k$ to $125b$ GHz for an unwanted sideband suppression over a dB, where the factor 125 is given considering that at the 1550-nm window, 1 nm in wavelength corresponds to 125 GHz

#159312 - $15.00 USD Received 2 Dec 2011; revised 29 Feb 2012; accepted 1 Mar 2012; published 6 Mar 2012

in frequency. For instance, the results shown in Fig. 2 are obtained using an optical filter with an edge slope of 230 dB/nm and a 1-dB bandwidth of 0.4 nm, so the system can generate an OSSB signal with a frequency varied from ~11 to 50 GHz (or 0.09-0.4 nm) for an unwanted sideband suppression over 20 dB. In addition, the optical filter is tunable from 1530 to 1610 nm, so the proposed OSSB modulator is very suitable for optical vector network analysis in which the wavelength of the optical carrier should be adjusted to measure the response of an optical component with a magnitude and phase response in a specific wavelength range.

To analyze the operation of the measurement system, we let the optical carrier signal be $\exp(j\omega_0 t)$ and the input RF signal to the PM be $\cos\omega_m t$. The optical field at the output of the optical filter can be written as

$$E(t) = e^{j\omega_0 t}\cdot e^{j\gamma\cos\omega_m t} \approx jkJ_1(\gamma)e^{j(\omega_0-\omega_m)t} + J_0(\gamma)e^{j\omega_0 t} + jJ_1(\gamma)e^{j(\omega_0+\omega_m)t} \quad (1)$$

where γ is the phase modulation index, $J_n(\gamma)$ (n = 0, 1) is the nth-order Bessel function of the first kind and k ($0\le k\le 1$) is a coefficient for the attenuation of the lower (or upper) sideband in the optical filter. The higher order (≥2) sidebands are ignored due to small signal modulation.

After the signal transmitted in a DUT with a transmission function of $H(\omega)$,we have

$$E'(\omega) = 2\pi jkJ_1(\gamma)H(\omega_0-\omega_m) + 2\pi J_0(\gamma)H(\omega_0) + 2\pi jJ_1(\gamma)H(\omega_0+\omega_m) \quad (2)$$

Sending the signal to a PD, and neglecting the J_1^2 term, we obtain the AC term of the current,

$$i_{AC}(\omega_m) \propto -4\pi^2 jkJ_0(\gamma)J_1(\gamma)H^*(\omega_0-\omega_m)H(\omega_0) + 4\pi^2 jJ_0(\gamma)J_1(\gamma)H^*(\omega_0)H(\omega_0+\omega_m) \quad (3)$$

If k = 1, which corresponds to the DSB modulation, Eq. (3) can be rewritten as

$$i_{AC}(\omega_m) \propto 4\pi^2 jJ_0(\gamma)J_1(\gamma)[H^*(\omega_0)H(\omega_0+\omega_m) - H^*(\omega_0-\omega_m)H(\omega_0)] \quad (4)$$

From Eq. (4), we can't recover $H(\omega)$. On the other hand, when k = 0, which corresponds to the SSB modulation, we can get the frequency response at $\omega_0 + \omega_m$,

$$H(\omega_0+\omega_m) \propto \frac{i_{AC}(\omega_m)}{4j\pi^2 J_0(\gamma)J_1(\gamma)H^*(\omega_0)} \quad (5)$$

Because $H(\omega_0)$ is a complex constant, and the term $4j\pi^2J_0(\gamma)J_1(\gamma)$ can be obtained by a calibration process, $H(\omega)$ around ω_0 can be measured by sweeping ω_m. Since in our implementation the OSSB can be achieved in a broad wavelength range, the transmission function of the DUT at different wavelengths can be accurately measured.

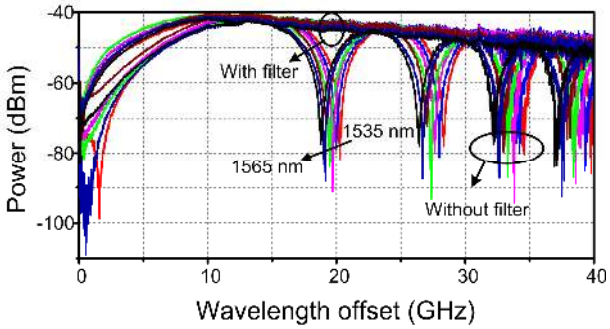

Fig. 3. The frequency responses of the ODSB (without filter) and OSSB (with filter) photonic link with 20-km SMF when the wavelength varied from 1535 to 1565nm. The response of the OSSB link is manually added by about 3 dB for a better comparison with that of the ODSB link.

#159312 - $15.00 USD Received 2 Dec 2011; revised 29 Feb 2012; accepted 1 Mar 2012; published 6 Mar 2012

3. Experimental demonstration

An experiment based on the setup shown in Fig. 1 is carried out. The TLS is an Agilent N7714A tunable laser source with a 24-hour wavelength drift of less than 2.5 pm and a linewidth of less than 100 kHz. The PM (EOSpace AZ-AV5-40) has a usable bandwidth of 40 GHz and a half-wave voltage of 4 V (measured at 1 GHz). The optical filter (Santec OTF-350) allows both wavelength tuning and passband width tuning independently. The tuning ranges of the passband width and the wavelength are 0.1-15 nm and 1530-1610 nm, respectively. The PD has a 3-dB bandwidth of 40 GHz and a responsivity of 0.65 A/V. A 40-GHz EVNA (Agilent N5230A) is used to measure the frequency response.

First we evaluate the SSB modulation, to do so, the signals before and after the optical filter are sent to a 20-km single-mode fiber (SMF). Figure 3 shows the frequency responses of the optical link with and without the optical filter when the optical wavelength varied from 1535 to 1565 nm. For the ODSB link, the fiber dispersion would introduce a frequency response given by $H(f_m) = \sin^2(\pi DL\lambda^2 f_m^2/c)$, where D and L are the dispersion parameter and the length of the SMF, λ is the carrier wavelength, f_m is the microwave frequency and c is the light velocity in vacuum. Deep notches are observed, as shown as the lower lines in Fig. 3. For the OSSB link, these notches do not exist. As can be seen from Fig. 3, the OSSB signal is immune to the fiber dispersion in the frequency range of 11-40 GHz for all the measured wavelengths from 1535 to 1565 nm. Therefore, an OSSB signal within a bandwidth of 29 GHz is generated. It should be noted that the magnitude in the frequency response is not constant, but is slightly decreasing with the frequency. This is caused due to the decreasing frequency responses of the PM and PD. As can be seen from Fig. 3, the frequency responses of SSB modulation are nearly unchanged even the carrier wavelength changes.

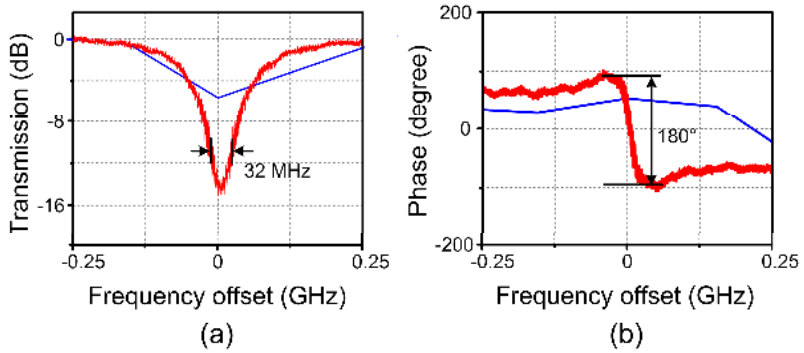

Fig. 4. The response of an ultra-narrow band phase-shifted FBG. (a) Magnitude response and (b) phase response of the phase-shifted FBG. Red line: measured by the proposed OVNA; blue line: measured by LUNA OVA CTe All Parameter Analyzer.

Then, we build the OVNA using the proposed OSSB modulator, and then use the OVNA to measure the frequency response of an ultra-narrow FBG. The FBG has a π-phase shift and is hyper-Gaussian apodized with an order 5 [14]. The frequency response of the phase-shifted FBG is shown in Fig. 4, where 6401 effective points are obtained over a span of 500 MHz, giving a resolution of 78 kHz. A frequency notch with a depth of 14 dB and a 3-dB bandwidth of 32 MHz are observed. The π-phase shift is also obtained in the phase response plot. Then, we compare the performance of this approach with the conventional interferometry method. To do so, we measure the magnitude and phase response of the phase-shifted FBG using a LUNA OVA CTe All Parameter Analyzer. The results are also shown in Fig. 4. As can be seen only three effective points (blue lines) over a span of 500 MHz are obtained, which corresponds to a resolution of 1.6 pm or 200 MHz. Due to the limited resolution, only a small magnitude notch and a small phase variation are observed.

#159312 - $15.00 USD Received 2 Dec 2011; revised 29 Feb 2012; accepted 1 Mar 2012; published 6 Mar 2012

The proposed OVNA can also be used to measure the spectral response of an active device. In our experiment, we use the OVNA to evaluate the SBS in a SMF of a length of 10.6-km. The SMF is pumped by laser diode at 1550.098 nm with the pump power increased from 2 to 16 dBm at a step of 2 dBm. Figure 5 shows the gain and phase responses of the SBS at different optical power levels. As can be seen, the gain and phase shift induced by the SBS effect increases as the pump power is increasing. The saturation effect is observed when the pump power is higher than 10 dBm. The measurement agrees very well with the theoretical analysis in [15].

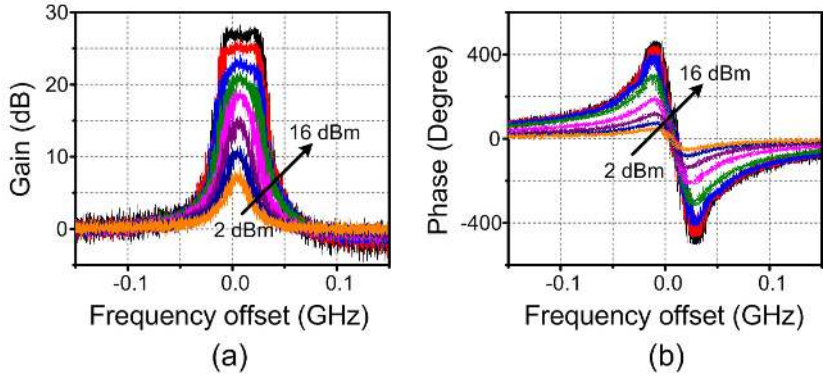

Fig. 5. The (a) gain and (b) phase responses of the SBS in a 10.6-km SMF when the pump power is increased from 2 to 16 dBm at a step of 2 dBm.

4. Conclusion

An approach to implementing a high resolution OVNA based on a wideband and wavelength-tunable OSSB modulator was proposed and experimentally demonstrated. The key to achieve high resolution optical vector network analysis is to use a wideband and high-resolution wavelength-tunable OSSB modulation, which was realized by using a PM and a tunable optical filter with a passband having steep edges and a flat top. The proposed OVNA was experimentally evaluated. The measurement of the magnitude and phase response of an ultra-narrow-band phase-shifted FBG and that of the SBS in a 10.6-km SMF was performed. A measurement resolution as high as 78 kHz was achieved.

Acknowledgments

The author would like to thank Masahito Hoshikawa for providing the tunable optical filter (Santec OTF-350). This work was supported in part by the National Natural Science Foundation of China under grant of 61107063, the Program for New Century Excellent Talents in University (NCET) under grant of NCET-10-0072, the National Basic Research Program of China (973 Program) under grant of 2012CB315705, the Ph.D. Programs Foundation of the Ministry of Education of China under grant of 20113218120018, and the Special Fund for Basic Scientific Research of Nanjing University of Aeronautics and Astronautics.

#159312 - $15.00 USD Received 2 Dec 2011; revised 29 Feb 2012; accepted 1 Mar 2012; published 6 Mar 2012